Solving Stochastic Orienteering Problems with Chance Constraints Using a GNN Powered Monte Carlo Tree Search

Marcos Abel Zuzuárregui Stefano Carpin

***Abstract*— Leveraging the power of a graph neural network (GNN) with message passing, we present a Monte Carlo Tree Search (MCTS) method to solve stochastic orienteering problems with chance constraints. While adhering to an assigned travel budget, the algorithm seeks to maximize collected reward while incurring stochastic travel costs. In this context, the acceptable probability of exceeding the assigned budget is expressed as a chance constraint. Our MCTS solution is an online and anytime algorithm, alternating planning and execution, that determines the next vertex to visit by continuously monitoring the remaining travel budget. The novelty of our work is that the rollout phase in the MCTS framework is implemented using a message-passing GNN, predicting both the utility and failure probability of each available action. This allows to enormously expedite the search process. Our experimental evaluation shows that with the proposed method and architecture, we manage to efficiently solve complex problem instances while incurring moderate losses in terms of collected reward. Moreover, we demonstrate how the approach is capable of generalizing beyond the characteristics of the training dataset. The paper's website, open-source code, and supplementary documentation can be found at `ucmercedrobotics.github.io/gnn-sop`.**

I. Introduction

Orienteering is an APX-hard optimization problem defined on a weighted graph, G, where each vertex has a reward and each edge has a non-negative cost [7]. The goal is to plan a path between designated start and end vertices to maximize the total reward collected from visited vertices while staying within a budget, B, that limits the total path length. This budget is often considered in terms of time, power, or distance that can be traveled (see Figure 1). Unlike the Traveling Salesman Problem (TSP), a typical solution to an orienteering problem instance does not visit all nodes. Instances of the orienteering problem can model various real-world scenarios we encounter daily, such as logistics [16], surveillance [14], [25], ridesharing [12], and precision agriculture [21], among others. Our interest in this problem is driven by its applications in precision agriculture [2], [18]–[20], though its range of uses is broad and continually expanding. Most research on orienteering has concentrated on the deterministic version, where both vertex rewards and edge costs are known in advance. However, this is not often the case in many practical scenarios. For example, when a robot moves from one location to another, the time or energy required for the movement is often a random variable rather than a deterministic value. This variant is known as the *stochastic orienteering problem* (SOP). Although SOP has been studied [1], it has received significantly less attention than its deterministic counterpart.

The authors are with the Department of Computer Science and Engineering, University of California, Merced, CA, USA. This work is partially supported by is partially supported by USDA-NIFA under award # 2021-67022-33452 (National Robotics Initiative) and by the IoT4Ag Engineering Research Center funded by the National Science Foundation (NSF) under NSF Cooperative Agreement Number EEC-1941529. Any opinions, findings, conclusions, or recommendations expressed in this publication are those of the author(s) and do not necessarily reflect the view of the U.S. Department of Agriculture or the National Science Foundation.

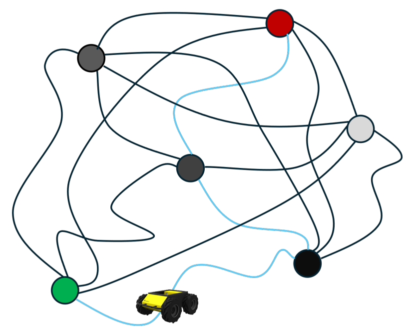

Fig. 1: The orienteering problem is defined on a graph G where vertices have rewards and edges have non-negative costs. The goal is to find a path from an assigned start vertex (the red node in this example) to a goal vertex (the green node) that maximizes the sum of collected rewards while ensuring the path cost does not exceed a given budget, B.

Recently, we proposed a novel solution to the stochastic orienteering problem using Monte Carlo Tree Search (MCTS), aimed at estimating both the collected reward and the probability of exceeding the allocated budget B [2]. Previous work highlighted in [24] and confirmed through our own experiments demonstrates that the rollout phase of MCTS can consume up to 99% of the total planning time. Aiming to accelerate the search with the goal of deploying a planner in applications requiring real-time response, in this work we investigate the potential of using a graph neural network (GNN) architecture to train a model capable of predicting rollout outcomes. A key innovation of our approach lies in simultaneously predicting two critical metrics needed to solve SOP instances: the accumulated reward and the probability of budget constraint violations. To the best of our knowledge, this dual prediction has not been explored previously.

Accordingly, in this contribution we present our GNN-powered MCTS SOP solver. Our novel contributions as follows:

- we introduce a single architecture capable of predicting values for a custom developed rollout procedure that can output action quality and failure probability;

- we demonstrate that this approach is competitive with the model that trained it and even optimal solutions, at times;
- we demonstrate that we can plan and execute complex orienteering solutions at real-time speeds.

The rest of the paper is organized as follows. Selected related work is presented in Section II. SOP is formalized in Section III, and in the same section we briefly define the model that generates our training data. The core of our contribution is in Section IV, where we describe the network we developed, as well as the feature attributes we identified to effectively train the networks. Extensive simulations detailing our findings are given in Section V, with conclusions and future work discussed in Section VI.

II. Related Literature

Early approaches to solve deterministic and stochastic orienteering problems relied on classical methods, often using heuristics due to the intrinsic computational complexity [8]. Notably, in [22] the authors propose an exact solution based on a mixed-integer linear program formulation to solve the stochastic orienteering problem with chance constraints. This approach is however offline, i.e., it computes a solution before execution starts and does not adapt on the fly. Our recent work [2] instead solves the problem using MCTS, designed to be an online method, whereby the vertices to visit are selected at runtime based on the remaining budget. This method, while competitive, devotes a significant amount of time to the rollout phase in MCTS search.

The practice of embedding policy and/or value networks into MCTS has been notably used in [15] and in subsequent papers such as [28]. Even though these papers do not use GNNs, they provide evidence of being able to solve computationally expensive problems by reducing the simulation required to approximate a solution. They leverage the power of MCTS and approximate their rollout phases, among other improvements. Several recent approaches have explored the use of GNN-based solutions to solve NP-hard graph optimization problems. For example, [5], [24] focused on using GNNs to solve TSP and other graph optimization problems. While different from orienteering, solutions to TSP are of interest due to some similarities in the problem formulation. Both of these papers used a message-passing framework with varying layer configurations. Importantly, [24] used MCTS to explore a limited horizon rather than the entire state space. In [11], the authors show that a similar implementation can be used to solve orienteering problems. In particular, a GNN-based approach is used in combination with a beam search method, as done in [24]. However, none of these approaches address stochastic orienteering. Equally relevant, to the best of our knowledge, no methods combining GNNs and MCTS have been developed to solve the SOP with chance constraints, which is the focus of this contribution.

III. Problem Statement and Background

In this section, we formally introduce the stochastic orienteering problem with chance constraints (SOPCC). We then outline our previous solution utilizing MCTS, which motivates the method proposed in this manuscript.

A. Stochastic Orienteering Problem with Chance Constraints

The deterministic orienteering problem is defined as follows. Let $G = (V, E)$ be a weighted graph with n vertices, where V is the set of vertices and E is the set of edges. Without loss of generality, we assume G is a complete graph. Define $r : V \to \mathbb{R}$ as the reward function assigning a reward to each vertex, and $c : E \to \mathbb{R}_+$ as the cost function assigning a positive cost to each edge. Let $v_s, v_g \in V$ be the designated start and end vertices, respectively, and let $B > 0$ be a fixed budget. Note that we allow $v_s = v_g$ for cases where the start and end vertices are the same. For a path P in G, define $R(P)$ as the sum of the rewards of the vertices along P, and $C(P)$ as the sum of the costs of the edges in P. The deterministic orienteering problem aims to find

$$P^* = \arg\max_{P \in \Pi} R(P) \qquad \text{s.t.} \;\; C(P^*) \leq B$$

where Π is the set of simple paths in G starting at v_s and ending at v_g. A simple path is defined as a path that does not revisit any vertex. Given the connectivity assumption of G, restricting Π to simple paths is not limiting. In the stochastic version of the problem, the cost associated with each edge is not fixed but rather sampled from a continuous random variable with a known probability density function that has strictly positive support. Specifically, for each edge $e \in E$ we assume $c(e)$ is sampled from $d(e)$ where $d(e)$ represents the random variable modeling the cost of traversing edge e. In general, different edges are associated with different random variables. In the stochastic case then, for a given path P the path cost $C(P)$ is also a random variable. The constraint on the path cost $C(P)$ must therefore be expressed using a chance constraint, defined formally as follows.

Stochastic Orienteering Problem with Chance Constraints (SOPCC) With the notation introduced above, let $0 < P_f < 1$ be an assigned failure bound. The SOPCC seeks to solve the following optimization problem:

$$P^* = \arg\max_{P \in \Pi} R(P)$$
$$\text{s.t. } \Pr[C(P^*) > B] \leq P_f.$$

Remark: Since the probability density functions of the random variables associated with the edges are assumed to be known, generating random samples for the cost $C(P)$ of a path P is straightforward and does not necessitate computing the probability density function of $C(P)$. This is consistent with the assumptions usually made when using MCTS to solve planning problems [9].

The problem definition models a decision maker aiming at maximizing the reward collected along a path while remaining below the allotted budget. Because the cost of the path $C(P)$ is a random variable, the constraint can be satisfied only in probability, and this leads to the introduction of the chance constraint $\Pr[C(P^*) > B] \leq P_f$.

B. Monte Carlo Tree Search for SOPCC

In [2], we introduced a new approach based on MCTS to solve the SOPCC. Key to our new solution was the introduction of a novel criterion for tree search dubbed UCTF – Upper Confidence Bound for Tree with Failures. In this subsection, we briefly review this solving method. We refer the reader to [2] for a deeper discussion of our method and to [4] for a general introduction to the MCTS methodology. Note that in [2], when deciding which vertex to add to the route, MCTS only considers the K-nearest neighbors to the current vertex. In the version implemented in this paper to train the GNN described in the next section, we remove this feature and instead consider all vertices. The reason is that in [2] we reduced the number of possibilities to expedite the online search, while here training is done offline. We can therefore consider a larger search space. As pointed out in [17] (chapter 8), a solution based on MCTS relies on the definition of four steps: selection, expansion, rollout, and backup. In the following, we sketch how these can be customized for solving SOPCC.

1) Selection: Selection, also known as the *tree policy*, guides the search from the root to a leaf node based on the value associated with the nodes in the tree. At every level, each child of the current node is evaluated using a metric, and the search then proceeds to the node with the highest value. Universal Confidence Bound for Trees (UCT) is commonly used to attribute values to nodes [10] and defines the tree policy. UCT, however, aims at maximizing reward only and is therefore not suitable for use in problems with chance constraints where high reward could lead to violations of the constraint. To overcome this limit, in [2] we introduced UCTF, defined as follows

$$UCTF(v_j) = Q[v_j](1 - F[v_j]) + z\sqrt{\frac{\log(N[v_p])}{N[v_j]}} \quad (1)$$

where the term $(1 - F[v_j])$ is new. In Eq. (1), $Q[v_i]$ is the estimate of how much reward will be collected by adding v_j to the route, $F[v_j]$ is a failure probability estimate for a path going through v_j, $N[v_j]$ is the number of times v_j has been explored, and $N[v_p]$ is the number of times its parent has been explored. Critically, in our original approach both Q and F are estimated via rollout, while in this paper we will train a GNN to quickly predict these values. The term $(1-F[v_j])$ penalizes nodes with high estimates for the failure value. As in the classic MCTS method, the term z balances exploration with exploitation.

2) Expansion: Expansion is the process of adding a node to the tree. In our implementation, this is implicitly obtained by assigning a UCTF value of infinity to vertices that are still unexplored (i.e., for which $N[v_j]$ is 0). This way, we ensure all children nodes of a parent node are explored at least once before one of the siblings is selected again.

3) Rollout: Once a node is added, rollout (also called simulation) is used to estimate the amount of reward that will be collected by going through that node as well as its failure probability. This is done by running a baseline, handcrafted, heuristic policy multiple times. The F value is estimated as the ratio of failed runs over total runs of the heuristic policy, while the Q value is estimated as the average of the returned value limited to the successful runs. A critical aspect of this step is the necessity of running the heuristic multiple times to numerically estimate F. In [2], the heuristic is a mix of random exploration and greedy search.

4) Backup: The backup step in [2] is unique because it propagates back not only the Q value, but also the F value. This is because for each action we must estimate not only the anticipated reward, Q, but also the probability, F, that the action will eventually result in a budget violation. To this end, two cases are considered by comparing the F value of the parent with the F value returned by the rollout. If the F value for the parent node v_p is $\leq P_f$, we check if the F value of the newly expanded node is also below P_f. If it is, we then compare the reward estimate, Q. If the child node has a larger estimate when adding the reward of the parent node, we update the parent estimate. If not, we move on. In the case where the parent node has an $F > P_f$, we check if the child node F estimate is less than the parent's. If it is, we update the parent's F and Q with F being the child's F value and Q being the child's Q plus the true, known reward of the parent node (see [2] for additional details).

IV. Methodology

A. MCTS Value and Failure Network

The main novelty of the method we propose here is a single value/failure network architecture that can be trained to predict either expected value, Q, or failure probability, F, of an action, v_j, to be used in the tree policy UCTF formula from Eq. (1). Therefore, after appropriate training, the MCTS rollout phase with multiple simulations to estimate both Q and F is replaced by a single forward pass on each network, thus dramatically cutting the computation time. As a result, as explained later, when a node is considered for expansion, all descendants are generated and evaluated at once. This is different from the classic MCTS approach where node descendants are added and evaluated one by one. This feature greatly extends the set of actions explored while not requiring more computational time.

B. Message Passing Neural Network

Given that orienteering problem instances are defined over graphs, a message passing neural network (MPNN) [26], [27] is the natural choice to implement the value and failure networks. MPNNs are graph neural networks in which, at every iteration of learning, nodes of the graph share information with neighboring nodes to generate a D-dimensional embedding for each node or for the entire graph. In a typical message passing framework, the message update function encompasses node attributes as well as edge attributes, both of which are critical in the SOPCC problem space. The following equations show the general relationship between an embedding and a message within the framework [6], formulated in terms of the aggregation operation given by

Eq. (2) (where the set $\mathcal{N}(v)$ is the set of nodes neighboring v) and the update operation given by Eq. (3).

$$m_v^{t+1} = \sum_{w \in N(v)} M_t(h_v^t, h_w^t, e_{vw}) \quad (2)$$

$$h_v^{t+1} = U_t(h_v^t, m_v^{t+1}) \quad (3)$$

Aggregation defines that a message m_v^{t+1} for node v at time $t+1$ is obtained by combining the embedding h_v^t with all of its neighbors' embeddings, h_w^t, at time t, as well as the attributes e_{vw} of the edges connecting them. The update operation then creates the embedding h_v^{t+1} for vertex v at time $t+1$ by combining its previous embedding at time t with the message at time $t+1$ obtained through aggregation. In both operations, it is assumed that the data is transformed by a function, i.e., M_t for aggregation and U_t for update. In our implementation, M_t is defined as a matrix multiplication between edge attribute linear transformations and node embeddings. This was defined in [6] as

$$M_t(h_v^t, h_w^t, e_{vw}) = A_{e_{vw}} h_w^t$$

The update function U_t is defined as a Gated Recurrent Unit (GRU) layer introduced in [3]. Note that [6] states that the GRU will take as input h_v^t and h_v^0 at every iteration, but we opt for the network from [13] which instead takes in h_v^t and h_v^{t-1}. This design choice was made after experimentally observing that the latter gives better results than the former. Finally, we pass the output from the message passing layers into a multi-layer perceptron (MLP) to obtain the Q and F values. In our implementation, we use three message passing layers, i.e., the maximum value for t is three. Critical to the approach are the node attributes to be used for h at time 0, as well as the edge attributes e_{vw} prior to linearization. These attributes will be defined in the remainder of this section. In our use case, we create two different networks using this architecture, one for Q and one for F[1]. We have two separate networks since the MCTS training data is best captured by two different activation functions for Q and F, We select a linear activation function for the Q value and a sigmoid for F. The reasoning is that Q predicts a positive, but potentially unbounded scalar value while F predicts a probability between 0 and 1. We also hypothesized that the networks would train differently on both types of labels, so we opted to separate them. Indeed, preliminary experiments showed that our loss was reduced when separating the models completely instead of having one model with two output activation functions or two output MLPs. We selected mean squared error (MSE) as the loss function for both Q and F outputs, as the task at hand is regression.

C. Attributes

For each node in the graph, we introduce an eight dimensional vector of attributes that will be used to define h_v in Eq. (2) for $t = 0$. Each node has the following attributes:

- a binary value indicating if the vertex has been visited;
- its x and y coordinates in the plane;
- its reward;
- the remaining budget;
- a binary value indicating if the node is the start vertex;
- a binary value indicating if the node is the end vertex;
- a binary value indicating if the node is the vertex where the robot is currently positioned at.

Our choice for these attributes is inspired by [24], where a similar approach was used to solve the TSP. Accordingly, the first three attributes provide the model with spatial awareness, which proved effective in TSP setting. However, since SOPCC has more constraints than TSP, we added additional attributes such as reward and residual budget. This is due to the fact that the nodes are not all uniformly important, and in general the agent will not be able to visit every node. Intuitively, incorporating more spatial and temporal information helps the model learn the greedy heuristic described in Section III-B. Indeed, as we will show in Section V-B through an ablation study, these additions were critical to achieving performance comparable to previous methods. For edge attributes e_{vw}, we set the single attribute to the Euclidean distance between nodes v and w. Note that the edge attributes do not include any information about the length variability $d(e_{v,w})$. This choice was based on preliminary tests, which showed no conclusive performance improvement from including this information. Additionally, omitting it reduces the number of model parameters, enabling a smaller training dataset and reducing training time.

In selecting our model architecture, we drew from the literature reviewed in Section II as well as a direct comparison using test cases. We trained both a Message Passing Neural Network (MPNN) [6] and a Graph Attention Network (GAT) [23]. Our initial hypothesis was that the attention mechanism in the GAT might help identify more valuable nodes by assigning higher weights to more promising neighbors. However, in practice, the GAT underperformed slightly compared to the MPNN. Specifically, the average reward achieved by the GAT was approximately 10% lower than that of our largest MPNN model, with only a marginal computational speedup of about 50 ms over the entire MCTS pipeline, including inference. This trade-off was not significant enough to justify selecting the GAT. Therefore, we opted for the neural message passing model presented in [6], [13], prioritizing its performance and training stability. Notably, the implementation from [13] includes a skip connection from the initial node attributes to the post-message-passing layers. We removed this skip layer to align more closely with the original design in [6] and because it did not result in any performance improvements in our experiments.

D. Training

To replace the rollout phase in MCTS with a trained model capable of estimating both utility (Q) and failure probability (F) without simulation, a necessary preliminary step is the generation of training data for the MPNN. To this end, we solved randomly generated instances of the SOPCC using the

[1]The complete GNN architecture as well as relevant training documentation can be found at `ucmercedrobotics.github.io/gnn-sop`.

MCTS algorithm described in Section III-B. These instances are defined over complete graphs, where rewards and (x, y) coordinates are independently and uniformly sampled from the interval $[0, 1]$ (see Figure 2), and edge lengths correspond to Euclidean distances. For training, we generated problem instances with 20, 30, and 40 vertices.

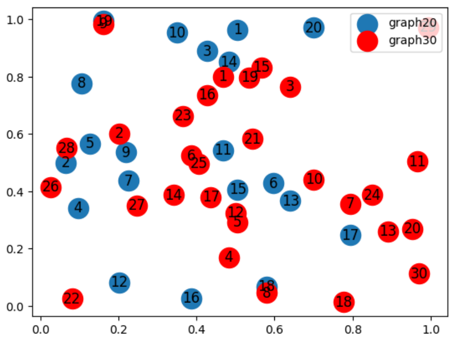

Fig. 2: Examples of randomly generated training graphs with twenty and thirty vertices.

We trained all of our networks using a budget of $B = 2$ and a failure probability of $P_f = 0.1$. During training, travel costs along edges were sampled from an exponential distribution with a mean equal to the deterministic edge length (the same noise model used in our preliminary work [2]). We observed that any network trained on more than 6,000 problem instance solutions appeared to converge, with the entire model size being 8.4 MB. Importantly, training data included only successful SOPCC solutions, i.e., cases where the MCTS algorithm produced routes that did not violate the budget constraint. We discuss the impact of these decisions in Section V.

V. Results

A. Experiments

We experimentally evaluated the performance of our GNN-MCTS architecture in predicting the Q and F values for efficiently solving SOPCC instances. We compare our method against an exact approach based on mixed integer linear programming [22] (referred to as MILP), as well as our previously proposed method in [2], referred to as MCTS-SOPCC. Additionally, for completeness, we include comparisons against the MCTS method described in Section III-B used during training and sharing similarities with MCTS-SOPCC but with minor implementation differences.

Our implementation is in Python 3.11.5, leveraging [13] for GNN layers. Tests were conducted on a machine with an Intel Core i7-10700F (2.90 GHz), 64 GB RAM, and an Nvidia 1660 SUPER GPU. The MILP solutions were obtained using the commercial solver Gurobi.

The main objective is to assess the value network's capability to learn heuristics and generalize across SOPCC instances of varying complexity. Compared to existing solvers, GNN-MCTS is expected to offer significant speed advantages and better scalability as problem size increases.

For fair comparison, both MCTS and MCTS-SOPCC use 100 rollouts ($S = 100$) to estimate Q and F values by averaging results from 100 independent executions, consistent with [2]. The search trees in these methods are expanded 350 times, also following [2]. In all experiments, the failure probability threshold is set to $P_f = 0.1$.

The results in Table I show graphs with different numbers of vertices and their associated MCTS timing breakdowns. The most evident result from these experiments is how linearly the rollout timing scales with size, and even improves, on average, as graph size grows. This improvement is due to the single forward pass used to approximate utility and failure chance for all nodes in the graph at once. Note that we observe the standard deviation of average rollout times for the GNN-MCTS large due to the single forward pass, which is averaged out over time until the next required forward pass, after all children have been evaluated from a single node. As shown in Table II, we see that the reward performance is very close while saving upwards of 1000% in overall timing, with similar results as complexity scales.

Timing aside, when solving SOPCC instances, one must consider both the reward collected and the failure rate. Accordingly, we define performance through two variables: the average reward obtained per solution, R, and the average rate of failure, F. Obviously, a method that collects high rewards but significantly exceeds the failure threshold P_f is not practically valuable. Hence, a viable solution is one that remains within the constraints while maximizing cumulative rewards. For this test, and those that follow, we reused the same test graphs supplied by [2] for benchmarking, in addition to larger graphs. Since we trained on instances with $P_f = 0.1$, we compare all methods using the same threshold. As shown in Table II, GNN-MCTS is, at times, more conservative and achieves lower failure rates F, while incurring only limited reward loss. However, in the case of larger, previously unseen graph sizes, we observe higher failure rates. We will further discuss the implications of network generalization in Section V-C.

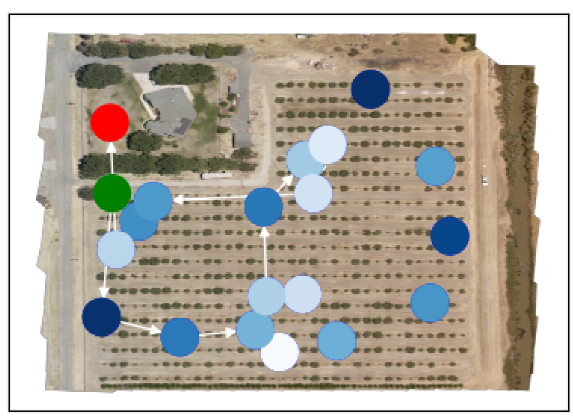

Fig. 3: A test case of size 20 plotted over our test orchard. The white arrows indicate what our GNN-MCTS solved for this problem as the best path.

	GNN-MCTS Timing Splits			
	Select (s)	Expand (s)	Rollout (s)	Backpropagate (s)
graph20$_{B=2}$	$8.6 \times 10^{-7} \pm 1.2 \times 10^{-7}$	$0.0002 \pm 1.7 \times 10^{-5}$	$\mathbf{0.001 \pm 0.007}$	$4.3 \times 10^{-5} \pm 6.7 \times 10^{-6}$
graph30$_{B=2}$	$1.0 \times 10^{-6} \pm 2.3 \times 10^{-7}$	$0.0002 \pm 1.4 \times 10^{-5}$	$\mathbf{0.001 \pm 0.006}$	$5.2 \times 10^{-5} \pm 8.3 \times 10^{-6}$
graph40$_{B=2}$	$1.1 \times 10^{-6} \pm 1.2 \times 10^{-7}$	$0.0002 \pm 2.1 \times 10^{-5}$	$\mathbf{0.0009 \pm 0.005}$	$6.3 \times 10^{-5} \pm 3.4 \times 10^{-6}$

	MCTS Timing Splits			
	Select (s)	Expand (s)	Rollout (s)	Backpropagate (s)
graph20$_{B=2}$	$2.3 \times 10^{-6} \pm 8.7 \times 10^{-7}$	$0.0002 \pm 2.6 \times 10^{-5}$	$\mathbf{0.002 \pm 0.001}$	$4.5 \times 10^{-5} \pm 1.2 \times 10^{-5}$
graph30$_{B=2}$	$2.3 \times 10^{-6} \pm 7.7 \times 10^{-7}$	$0.0002 \pm 3.0 \times 10^{-5}$	$\mathbf{0.011 \pm 0.008}$	$5.3 \times 10^{-5} \pm 2.3 \times 10^{-5}$
graph40$_{B=2}$	$2.7 \times 10^{-6} \pm 7.8 \times 10^{-7}$	$0.0003 \pm 3.7 \times 10^{-5}$	$\mathbf{0.020 \pm 0.014}$	$6.4 \times 10^{-5} \pm 1.5 \times 10^{-5}$

TABLE I: Timing breakdown between MCTS with and without GNN value network over 100 trials.

In Table III, we display the performance ratios between GNN-MCTS, the MCTS model used to generate its training data, and the MILP solver. This illustrates how remarkably fast and effective our model is compared to existing methods. We stay within 93% or better of our MCTS model, demonstrating that this architecture loses less than 10% performance in these cases. Even more impressively, in some cases we outperform the original model. While performance against the MILP achieves 60% or better in terms of reward, we expect improvements with optimal training data—which is significantly more difficult and time-consuming to generate. Figure 4 compares the solutions produced by three of the evaluated algorithms for an SOPCC instance with 40 vertices.

It is also interesting to explore how the solver performs as P_f varies. While in most cases, model performance characterized by P_f was as expected, a limitation of our implementation is that the activation function modeling F is a sigmoid, which does not fully capture failure as a function.

Ultimately, we achieved real-time approximation results in a stochastic environment. Figure 3 shows the solution produced by GNN-MCTS while solving an instance of SOPCC associated with a sampling problem in precision agriculture. The blue dots represent locations to visit, with the color intensity indicating the reward (darker means higher reward). The robot starts at the green vertex and must end at the red vertex before running out of budget.

B. Ablation Study

Previous literature has shown that including spatial information in vertex attributes is essential for evaluating the effectiveness of GNN-based methods on problems like the TSP [5]. However, because SOPCC solutions are also influenced by rewards, remaining budget, and the start and goal locations, as discussed in Section IV-C, we extended the attribute set accordingly in our implementation. This subsection presents an ablation study to assess the impact of our novel temporal and spatial attribute additions, specifically the one-hot encoding of the currently visited vertex and the start/goal vertices.

In Figure 5, we see that removing any of the additional attributes results in a decrease in average reward. In the case of removing the start/end vertex attribute, we observed nearly a 50% loss in reward. However, the most significant impact is on the failure rate, which exceeds the P_f constraint and renders the solution infeasible. The same figure also shows that omitting the current vertex attribute does not lead to a violation of P_f, but the average total reward is worse than that of the original model. While this solution is more conservative, achieving a lower F rate, our original model maintains compliance with P_f while collecting, on average, more reward.

For node-level classification using GNNs, these findings are relatively significant: GNNs can capture temporal and spatial relationships relevant to a given problem. Rather than embedding this information elsewhere in the algorithm, we can instead task the GNN with learning explicitly defined spatiotemporal data.

C. Generalization

As with any learning-based approach, the quality of the solution depends heavily on the nature of the training dataset. In our work, with the explicit goal of assessing the model's ability to learn and generalize, we trained using a fixed failure probability $P_f = 0.1$ and budget $B = 2$, employing the same underlying graph topology, i.e., complete graphs with vertices uniformly distributed in the unit square. Given these premises, it is essential to evaluate how well the proposed architecture generalizes to instances characterized by new parameters. We investigated generalization from two perspectives: varying graph sizes and previously unseen budgets. The ability to generalize across these parameters is important not only for robustness but also to accelerate training, particularly with respect to graph size, since larger instances require significantly more time to generate solutions using the MCTS algorithm employed during training. As noted in Section IV-D, our training data consisted solely of graphs with 20, 30, and 40 vertices.

For generalization with respect to size, we observed in Table II that within a certain size range, the model delivers equally competitive performance. For example, we pushed our model to the high end of what is seen in the SOPCC literature (e.g., up to 70 vertices) and found that generalization is quite effective in terms of reward performance. However, due to the sigmoid issue described earlier, for larger problem instances the model requires tuning of the P_f value. Specifically, as shown in Table II, when feeding the model a desired P_f value for unseen problem instances, the solutions can have failure probabilities that significantly exceed the limit. This issue can be remedied by providing the model with a P_f value smaller than the desired one. Note that this hyperparameter tuning process is also necessary when

	P_f	GNN-MCTS			MCTS			MCTS-SOPCC			MILP		
		Reward	Time (s)	F	Reward	Time (s)	F	Reward	Time (s)	F	Reward	Time (s)	F
graph20$_{B=2}$	0.1	2.762	0.226	4%	2.967	5.092	10%	3.49	10.99	11%	3.414	316.16	12%
graph30$_{B=2}$	0.1	5.675	0.442	10%	5.517	43.969	12%	6.433	23.117	7%	6.973	9.949	10%
graph40$_{B=2}$	0.1	5.523	0.447	13%	5.75	70.712	11%	8.052	43.698	10%	8.843	457.13	10%
graph20$_{B=3}$$^{\&}$	0.1	4.27	0.329	4%	4.207	7.003	7%	5.481	26.64	13%	5.404	601.078	14%
graph30$_{B=3}$$^{\&}$	0.1	6.519	0.483	7%	6.804	59.63	14%	7.934	47.848	11%	8.779	317.093	10%
graph40$_{B=3}$$^{\&}$	0.1	7.106	0.555	1%	7.343	99.019	13%	10.434	77.774	12%	11.548	600.609	14%
graph50$_{B=2}$*	0.1	6.952	0.533	18%$^{!}$	6.422	45.935	10%	8.394	26.06	4%	9.019	600.79	13%
graph60$_{B=2}$*	0.1	8.889	0.756	30%$^{!}$	7.429	148.93	11%	10.29	31.031	10%	10.602	601.09	10%
graph70$_{B=2}$*	0.1	8.462	0.778	40%$^{!}$	8.381	205.451	12%	11.721	31.222	11%	12.35	601.459	10%

TABLE II: Overall results from benchmarks used in [2] plus even larger graphs averaged over 100 trials. Top rows are for results against previously seen budgets. * signify tests run with a model trained against size 40 graphs. $^{\&}$ are for results against unseen budgets using same sized model. $^{!}$ is further explained in V-C.

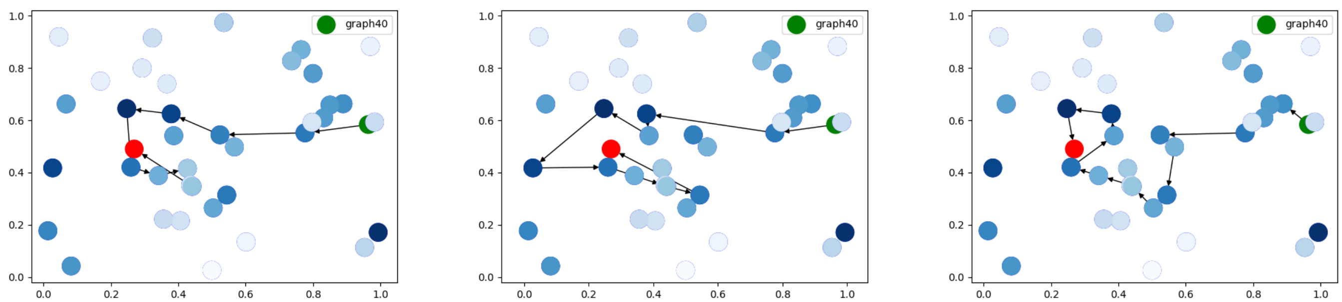

(a) Graph40 GNN-MCTS solution (b) Graph40 MCTS solution (c) Graph40 MILP solution

Fig. 4: Proposed solutions for three algorithms graph40 test described in Table II. The green node is start; red is goal. The blue represents nodes of varying reward, darker being higher.

	GNN-MCTS / MILP		GNN-MCTS / MCTS	
	R Ratio	Time Ratio	R Ratio	Time Ratio
graph20$_{B=2}$	0.809	1428.57	0.931	22.73
graph30$_{B=2}$	0.814	22.73	1.029	100.00
graph40$_{B=2}$	0.625	1111.11	0.961	158.73
graph20$_{B=3}$	0.79	2000.00	1.015	21.28
graph30$_{B=3}$	0.743	666.67	0.958	123.46
graph40$_{B=3}$	0.615	1075.27	0.968	178.57

TABLE III: Ratios between our solver and baseline solvers for reward and time averaged over 100 trials. See Table IV for unseen graph sizes.

	P_f	R	MCTS R Ratio	F
graph50$_{B=2}$	0.075	6.171	0.961	6%
graph60$_{B=2}$	0.06	7.531	1.014	8%
graph70$_{B=2}$	0.075	8.007	0.955	7%

TABLE IV: When hyperparameterizing P_f on unseen graph sizes, we see the model performance improve to near ground truth, presumably due to the sigmoid activation function.

using the exact method [22] and is not a limitation unique to our method. Table IV demonstrates how, by adjusting the P_f value in unseen problem instances, GNN-MCTS successfully meets the originally desired failure rate.

In the case of budget generalization, as shown in Table II, our method was able to maintain similar time and performance ratios, detailed in Table III, for unseen budgets. Given that solving a SOP with a lower budget is more difficult, it makes sense that providing more budget simplifies the task for the model. However, we observe our algorithm exhibiting noticeably lower failure rates, F, without sacrificing reward, R, implying once again that our method is more conservative without a significant performance impact.

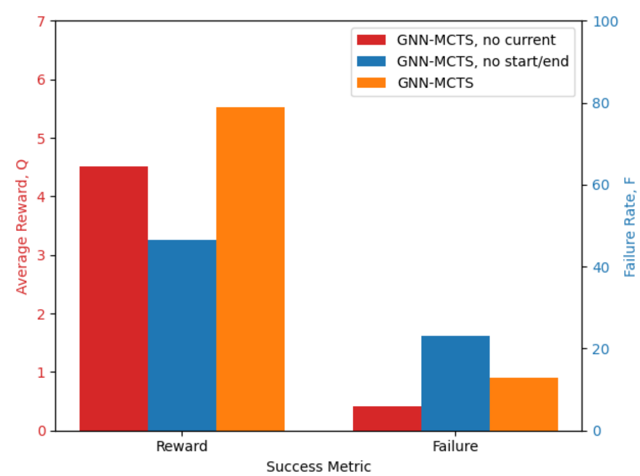

Fig. 5: Ablation study substantiating that both temporal and spatial node attribute additions are needed for the value network to perform effectively as removing either one implies decrease in reward collected (left) or increase in failure rate (right). Data averaged over 100 trials with $P_f = 0.1$.

VI. Conclusions and Future Work

In this paper, we have presented a novel solution to the SOPCC by combining MCTS with a message passing graph neural network. This is achieved by training a neural network to replace the computationally expensive rollout phase in MCTS. Building on the key idea introduced in [2], the trained model simultaneously predicts both the expected collected reward, Q, and the predicted failure probability, F. This capability was not found in previous works employing value networks with reinforcement learning. Another advantage of our methodology is that, during the expansion phase, a single forward pass of the network predicts values for all child nodes simultaneously, rather than evaluating them one by one. This enables the algorithm to efficiently explore a larger portion of the search space.

Our method was trained using SOPCC solutions generated by a slightly modified version of the algorithm presented in [2]. Extensive simulations compared this new approach against the training method, our previous MCTS algorithm [2], and an exact MILP-based solution. The results demonstrate that our proposed method is orders of magnitude faster while satisfying the failure constraint and preserving a significant portion of the collected reward, though some hyperparameter tuning may be required in certain cases. Our ablation study further confirms that the selected vertex attributes for the embeddings are critical to the method's success.

There are numerous directions for current and future work. First, it would be interesting to train the model using solutions generated by different heuristics or even an ensemble of heuristics to assess whether this improves overall performance, especially in generalizing to larger problem instances. We also plan to explore applying this model, either in centralized or distributed settings, to multi-robot problems involving communication. Additionally, investigating alternative vertex or edge attributes may enhance the predictive capabilities of the network. Similarly, modifications to the network's final layers, such as improved activation functions, could yield better results. Finally, we are currently implementing the planner in ROS 2 and integrating it into our autonomous navigation stack for precision agriculture, assessing its real-time applicability to complex data collection problems in the field.

References

[1] A.M. Campbell, M. Gendreau, and B.W. Thomas. The orienteering problem with stochastic travel and service times. *Annals of Operations Research*, 186(1):61–81, 2011.

[2] S. Carpin. Solving stochastic orienteering problems with chance constraints using monte carlo tree search. *IEEE Transactions on Automation Science and Engineering*, 22:7855–7869,, 2025.

[3] K. Cho, B. van Merrienboer, D. Bahdanau, and Y. Bengio. Learning phrase representations using RNN encoder–decoder for statistical machine translation. In *Proceedings of the Conference on Empirical Methods in Natural Language Processing*, pages 1724–1734, 2014.

[4] Rémi Coulom. Efficient selectivity and backup operators in monte-carlo tree search. In H. Jaap van den Herik, Paolo Ciancarini, and H. H. L. M. Donkers, editors, *Computers and Games, 5th International Conference, CG 2006, Turin, Italy, May 29–31, 2006. Revised Papers*, pages 72–83. Springer, 2007.

[5] H. Dai, E.B. Khalil, Y. Zhang, B. Dilkina, and L. Song. Learning combinatorial optimization algorithms over graphs. In *Proceedings of the 31st International Conference on Neural Information Processing Systems*, pages 6351 – 6361, 2017.

[6] J. Gilmer, S.S. Schoenholz, P.F. Riley, O. Vinyals, and G.E. Dahl. Neural message passing for quantum chemistry. In *Proc. of the Intnl. Conf. on Machine Learning*, pages 1263–1272, 2017.

[7] B. L. Golden, L. Levy, and R. Vohra. The orienteering problem. *Naval Research Logistics*, 34:307–318, 1987.

[8] A. Gunawan, H. C. Lau, and P. Vansteenwegen. Orienteering problem: A survey of recent variants, solution approaches, and applications. *European Journal of Operational Research*, 255(2):315–332, 2016.

[9] A. Gupta, R. Krishnaswamy, V. Nagarajan, and R. Ravi. Running Errands in Time: Approximation Algorithms for Stochastic Orienteering. *Mathematics of Operations Research*, 40(1):56–79, February 2015. Publisher: INFORMS.

[10] L. Kocsis and C. Szepesvári. Bandit based monte-carlo planning. In *Machine Learning: ECML 2006*, pages 282–293, 2006.

[11] Z. Liu, W. Dong, C. Wang, H. Shen, G. Sun, Q. Jiang, Q. Tao, and Y. Yang. Boosting graph search with attention network for solving the general orienteering problem. *AI Open*, 5:46–54, 2024.

[12] L. Martin, S. Minner, D. Pocas, and A.S. Schultz. The competitive pickup and delivery orienteering problem for balancing car-sharing systems. *Transportation Science*, 55(6):1232–1259, 2021.

[13] P. Reiser, A. Eberhard, and P. Friederich. Graph neural networks in TensorFlow-Keras with RaggedTensor representation (kgcnn). *Software Impacts*, page 100095, 2021.

[14] G. Shi, L. Zhou, and P. Tokekar. Robust multiple-path orienteering problem: Securing against adversarial attacks. *IEEE Transactions on Robotics*, 39(3):2060–2077, 2023.

[15] D. Silver, J. Schrittwieser, K. Simonyan, I. Antonoglou, A. Huang, A. Guez, T. Hubert, L. Baker, M. Lai, A. Bolton, Y. Chen, T. Lillicrap, F. Hui, L. Sifre, G. van den Driessche, T. Graepel, and D. Hassabis. Mastering the game of go without human knowledge. *Nature*, 550(7676):354–359, 2017.

[16] F. Betti Sorbelli, S. Carpin, F. Coró, S.K. Das, A. Navarra, and C.M. Pinotti. Speeding up routing schedules on aisle-graphs with single access. *IEEE Transactions on Robotics*, 38(1):433–447, 2022.

[17] R.S. Sutton and A.G. Barto. *Reinforcement Learning – an introduction*. MIT Press, 2nd edition, 2018.

[18] T.C. Thayer and S. Carpin. Solving large-scale stochastic orienteering problems with aggregation. In *Proceedings of the IEEE/RSJ International Conference on Intelligent Robots and Systems*, pages 2452–2458, 2020.

[19] T.C. Thayer and S. Carpin. An adaptive method for the stochastic orienteering problem. *IEEE Robotics and Automation Letters*, 6(2):4185–4192, 2021.

[20] T.C. Thayer and S. Carpin. A fast algorithm for stochastic orienteering with chance constraints. In *Proceedings of the IEEE/RSJ International Conference on Intelligent Robots and Systems*, pages 7961–7968, 2021.

[21] T.C. Thayer, S. Vougioukas, K. Goldberg, and S. Carpin. Multirobot routing algorithms for robots operating in vineyards. *IEEE Transactions on Automation Science and Engineering*, 17(3):1184–1194, 2020.

[22] P. Varakantham and A. Kumar. Optimization approaches for solving chance constrained stochastic orienteering problems. In Patrice Perny, Marc Pirlot, and Alexis Tsoukiàs, editors, *Algorithmic Decision Theory*, pages 387–398, Berlin, Heidelberg, 2013. Springer Berlin Heidelberg.

[23] P. Veličković, G. Cucurull, A. Casanova, A. Romero, P. Liò, and Y. Bengio. Graph attention networks. *CoRR*, abs/1710.10903, 2018.

[24] Z. Xing and S. Tu. A graph neural network assisted monte carlo tree search approach to traveling salesman problem. *IEEE Access*, 8:108418–108428, 2020.

[25] J. Yu, M. Schwager, and D. Rus. Correlated orienteering problem and its application to persistent monitoring tasks. *IEEE Transactions on Robotics*, 32(5):1106–1118, 2016.

[26] J. Zhou, G. Cui, Z. Zhang, C. Yang, Z. Liu, and M. Sun. Graph neural networks: A review of methods and applications. *CoRR*, abs/1812.08434, 2018.

[27] Z.Wu, S. Pan, F. Chen, G. Long, C. Zhang, and P. S. Yu. A comprehensive survey on graph neural networks. *CoRR*, abs/1901.00596, 2019.

[28] M. Świechowski, T. Tajmajer, and A. Janusz. Improving hearthstone ai by combining mcts and supervised learning algorithms. In *Proceedings of the IEEE Conference on Computational Intelligence and Games*, pages 1–8, 2018.